aid of (2.10) and (2.11):

$$\frac{a_1-b_1}{a_1+b_1}+n_0\frac{a_2-b_2}{a_1+b_1}+\frac{a_3^2-b_3^2}{(a_1+b_1)^2}$$
$$=\beta\ln\left(\frac{r_3}{r_1}\right)\left\{\sum_{P=1}^{\infty}\left(\int_{r_2}^{r_3}E_\rho(\rho',0)\rho' Z_{PA}(\rho')\,d\rho'\right)^2\Big/\beta_{PA}\right.$$
$$\left.+\sum_{P=2}^{\infty}\left(\int_{r_2}^{r_3}E_\rho(\rho',0)\rho Z_{PB}(\rho')\,d\rho'\right)^2\Big/\beta_{PB}\right\}$$
$$\Big/\left(\int_{r_2}^{r_3}E_\rho(\rho',0)\,d\rho'\right)^2. \qquad \text{(A1.6)}$$

Now considering the case when $a_1=a_2=1$, and $a_3=0$ and denoting the total transverse electric field, at the junction, for this case by $\tilde{E}_\rho(\rho,0)$ we can obtain the variational relation (2.15a) with the aid of (2.13a) and (2.13b). In (2.15a) we recognize that the first term in the second infinite sum precisely corresponds to $\{b_3^2/(a_1+b_1)^2\}$ with $a_3=0$.

Considering the case when $a_1=(1-S_{33})/S_{13}$, $a_2=0$, and $a_3=1$ and denoting the total transverse electric field, at the junction, for this case by $\tilde{\tilde{E}}_\rho(\rho,0)$ we can obtain the second variational relation (2.15b).

ACKNOWLEDGMENT

The authors are very grateful to Dr. M. T. Ma and Dr. M. Kanda for their technical discussions and helpful suggestions during the course of this work. The cooperation and assistance received from M. Crawford is also acknowledged. The work reported herein would not have been possible without the constant support and encouragement from C. K. S. Miller and F. X. Ries.

REFERENCES

[1] J. R. Whinnery and H. W. Jamieson, "Equivalent circuits for discontinuities in transmission lines," *Proc. IRE*, vol. 32, pp. 98–114, Feb. 1944.
[2] J. R. Whinnery, H. W. Jamieson, and T. E. Robbins, "Coaxial line discontinuities," *Proc. IRE*, vol. 32, pp. 695–709, Nov. 1944.
[3] N. Marcuvitz, *Waveguide Handbook* (M.I.T. Rad. Lab. Series, vol. 10). New York: McGraw-Hill, 1951, pp. 229–238.
[4] R. N. Ghose, *Microwave Circuit Theory and Analysis*. New York: McGraw-Hill, 1963, pp. 302–314.
[5] M. L. Crawford, "Generation of standard EM field using TEM transmission cells," *IEEE Trans. Electromagn. Compat.*, vol. EMC-16, pp. 189–195, Nov. 1974.
[6] S. J. Mason, "Feedback theory—some properties of signal flow graphs," *Proc. IRE*, vol. 41, pp. 1144–1156, Sept. 1953.
[7] S. J. Mason, "Feedback theory—further properties of signal flow graphs," *Proc. IRE*, vol. 44, pp. 920–926, July 1956.
[8] R. E. Collins, *Field Theory of Guided Waves*. New York: McGraw-Hill, 1960, pp. 200–204.

Eigenvalue Spectrum of Rectangular Waveguide with Two Symmetrically Placed Double Ridges

D. DASGUPTA AND P. K. SAHA

Abstract—**The eigenvalue spectrum of rectangular waveguide with two symmetrically placed double ridges has been determined by formulating an integral eigenvalue problem and solving by Ritz–Galerkin method. The bandwidth characteristic is found to be adequate for varactor-tuned solid-state microwave oscillator applications requiring ridge structure for resonator. There remains some ambiguity in the designation of trough modes.**

I. INTRODUCTION

RIDGED WAVEGUIDES have many applications in microwave circuits because of their intrinsic broad bandwidth [1]–[3]. A rectangular waveguide with two symmetrically placed double ridges was proposed and used by Jull *et al.* [4] for microwave heating. The design data were presented in the form of normalized cutoff wavelength of the dominant TE mode for various ridge parameters. These were calculated by the five point finite difference method and extrapolated to the zero mesh limit. For the experimental verification measurements were also carried out on WR 340 waveguide with double ridges.

Among the other possible applications of such waveguides one appears to be in oscillators. Wide-band operation of Gunn oscillators using the conventional ridged waveguide has been demonstrated [5], [6]. The waveguide with two symmetrical double ridges may well be useful for the broad-band varactor-tuned Gunn oscillator with two

Manuscript received June 9, 1980; revised August 28, 1980.
The authors are with the Institute of Radiophysics and Electronics, 92, Acharya Prafulla Chandra Road, Calcutta-700009, India.

0018-9480/81/0100-0047$00.75 ©1981 IEEE

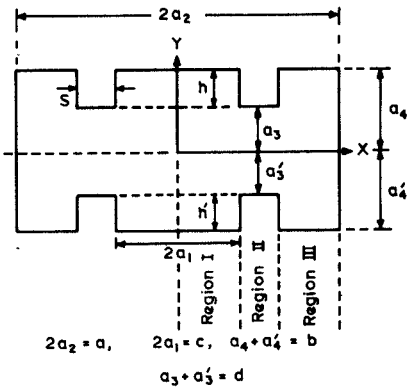

Fig. 1. Rectangular waveguide with two symmetrically placed double ridges-transverse plane.

diodes gap mounted in parallel. The calculations show that for the ridge parameters appropriate for such an application, this waveguide has a bandwidth of at least an octave. Whatever the application, one needs to know the complete eigenvalue spectrum of the waveguide. This has been evaluated following Montgomery's [7] work on ridged waveguide. An integral eigenvalue problem is formulated and solved numerically by Ritz–Galerkin method. The results of computation on the dominant as well as a few higher order modes are presented.

II. Formulation of the Problem

The geometry of the ridged waveguide is shown in Fig. 1 along with the dimensional notations. The only plane of symmetry assumed is the Y–Z plane. The problem can then be divided into four cases of TE and TM modes with the electric or magnetic wall at the plane of symmetry. The TE mode analysis is given in detail while for the TM mode the final matrix equations are given without derivation.

Using the notations of Montgomery [7] for convenience, the introductory equations for deriving the TE basis fields from the Hertzian vector π_h are written briefly as follows:

$$\pi_h = g(r_T)\phi(z)\hat{l}_z \tag{1}$$

where

$$(\nabla_t^2 + K_T^2)g(r_T) = 0$$

$$(\partial^2/\partial z^2 + \gamma^2)\phi(z) = 0 \tag{2}$$

$$\gamma = \sqrt{K_0^2 - K_T^2}, \qquad \text{if } K_0 = \frac{2\pi}{\lambda} > K_T$$

$$= -j\sqrt{K_T^2 - K_0^2}, \qquad \text{if } K_0 < K_T. \tag{3}$$

The TE basis fields are given by

$$e_T(r_T) = \nabla g(r_T) \times \hat{l}_z \tag{4}$$

$$h_T(r_T) = (\gamma/j\omega\mu_0)\hat{l}_z \times e_T(r_T). \tag{5}$$

Using the TE boundary conditions we can write the following expressions for $g(r_T)$ in the gap and trough regions.

A. Region I ($0 \leqslant x \leqslant a_1$)

$$g_1(r_T) = \sum_{m=0}^{\infty} \eta_{1m} \begin{matrix}\sin\\ \cos\end{matrix} K_{x1m} x \cos\frac{m\pi}{b}(y - a_4) \tag{6}$$

where the upper and lower functions correspond, respectively, to the magnetic and electric symmetry and

$$K_{x1m}^2 + \left(\frac{m\pi}{b}\right)^2 = K_T^2.$$

B. Region II ($a_1 \leqslant x \leqslant a_1 + s$)

$$g_2(r_T) = \sum_{n=0}^{\infty} \eta_{2n}(A \sin K_{x2n}x + B\cos K_{x2n}x)\cos\frac{n\pi}{d}(y - a_3)$$

$$\cdot K_{x2n}^2 + \left(\frac{n\pi}{d}\right)^2 = K_T^2. \tag{7}$$

C. Region III ($a_1 + s \leqslant x \leqslant a_2$)

$$g_3(r_T) = \sum_{l=0}^{\infty} \eta_{3l}\cos K_{x3l}(x - a_2)\cos\frac{l\pi}{b}(y - a_4)$$

$$K_{x3l}^2 + \left(\frac{l\pi}{b}\right)^2 = K_T^2. \tag{8}$$

From the condition $g_1 = g_2$ at the aperture at $x = a_1$ we obtain

$$\sum_{m=0}^{\infty} \eta_{1m} \begin{matrix}\sin\\ \cos\end{matrix} K_{x1m} a_1 \cos\frac{m\pi}{b}(y - a_4)$$

$$= \sum_{n=0}^{\infty} \eta_{2n}(A \sin K_{x2n}a_1 + B\cos K_{x2n}a_1)\cos\frac{n\pi}{d}(y - a_3). \tag{9}$$

Let $E_{g_1}(y)$ be the unknown aperture field at $x = a_1$. Then from the continuity of $e_y(r_T)$ at $x = a_1$ we obtain the following equations:

$$-\eta_{1m}K_{x1m}\left[\begin{matrix}\cos\\ -\sin\end{matrix} K_{x1m}a_1\right]\epsilon_m b =$$

$$\cdot \int_{-a_3'}^{a_3} E_{g_1}(y')\cos\frac{m\pi}{b}(y' - a_4)\,dy' \tag{10}$$

and

$$-\eta_{2n}K_{x2n}(A\cos K_{x2n}a_1 - B\sin K_{x2n}a_1)\epsilon_n d = \int_{-a_3'}^{a_3} E_{g_1}(y')\cos\frac{n\pi}{d}(y'-a_3)\,dy' \quad (11)$$

where

$$\epsilon_n = 1, \quad \text{for } n=0$$
$$= 1/2, \quad \text{for } n\neq 0.$$

Proceeding similarly with the boundary conditions at $x = a_1+s$ and denoting the unknown transverse electric field at the aperture by $E_{g_2}(y)$, the following equations are obtained:

$$\sum_{n=0}^{\infty}\eta_{2n}[A\sin K_{x2n}(a_1+s)+B\cos K_{x2n}(a_1+s)]\cdot\cos\frac{n\pi}{d}(y-a_3) = \sum_{l=0}^{\infty}\eta_{3l}\cos K_{x3l}(a_1+s-a_2)\cos\frac{l\pi}{b}(y-a_4) \quad (12)$$

$$-\eta_{2n}K_{x2n}[A\cos K_{x2n}(a_1+s)-B\sin K_{x2n}(a_1+s)]\epsilon_n d = \int_{-a_3'}^{a_3} E_{g_2}(y')\cos\frac{n\pi}{d}(y'-a_3)\,dy' \quad (13)$$

$$\eta_{3l}K_{x3l}\sin K_{x3l}(a_1+s-a_2)\epsilon_l b = \int_{-a_3'}^{a_3} E_{g_2}(y')\cdot\cos\frac{l\pi}{b}(y'-a_4)\,dy'. \quad (14)$$

Substituting for η_{1m} and η_{3l} in (9) and (12) from (10) and (14), respectively, and solving $\eta_{2n}A$ and η_{2nB} from (11) and (13) we obtain the following coupled equations:

$$-\sum_{m=0}^{\infty}\frac{\tan}{-\cot}\frac{K_{x1m}a_1}{\epsilon_m bK_{x1m}}\cos\frac{m\pi}{b}(y-a_4)\cdot\int_{-a_3'}^{a_3}E_{g_1}(y')\cos\frac{m\pi}{b}(y'-a_4)\,dy' = \sum_{n=0}^{\infty}\left(\frac{F_{g_2}-F_{g_1}\cos K_{x2n}s}{\epsilon_n dK_{x2n}\sin K_{x2n}s}\right)\cos\frac{n\pi}{d}(y-a_3) \quad (15)$$

$$\sum_{l=0}^{\infty}\frac{\cot K_{x3l}(a_1+s-a_2)}{\epsilon_l bK_{x3l}}\cos\frac{l\pi}{b}(y-a_4)\cdot\int_{-a_3'}^{a_3}E_{g_2}(y')\cos\frac{l\pi}{b}(y'-a_4)\,dy' = \sum_{n=0}^{\infty}\left(\frac{F_{g_2}\cos K_{x2n}s-F_{g_1}}{\epsilon_n dK_{x2n}\sin K_{x2n}s}\right)\cos\frac{n\pi}{d}(y-a_3) \quad (16)$$

where F_{g_1} and F_{g_2} represent the right-hand sides of (11) and (13), respectively. For solving these equations $E_{g_1}(y)$ and $E_{g_2}(y)$ are expanded as

$$E_{g_1}(y) = \sum_{i=0}^{I_1} C_i\cos\frac{i\pi}{d}(y-a_3) \quad (17)$$

and

$$E_{g_2}(y) = \sum_{i=0}^{I_2} D_i\cos\frac{i\pi}{d}(y-a_3). \quad (18)$$

These are substituted in (15) and (16) and inner product is taken with $\cos q\pi(y-a_3)/d$, $q=0,1,2,\cdots,Q$. On defining a coefficient P_{rs} as

$$P_{rs} = \int_{-a_3'}^{a_3}\cos\frac{r\pi}{d}(y-a_3)\cos\frac{s\pi}{b}(y-a_4)\,dy \quad (19)$$

and truncating the m- and l-summations to $M+1$ and $L+1$ terms, respectively, (15) and (16) yield the following matrix equations:

$$[U_1][C]+[V_1][D]=0 \quad (20)$$

$$[U_2][C]+[V_2][D]=0 \quad (21)$$

where $[C]$ and $[D]$ are column vectors and $[U_1],[V_1],[U_2],[V_2]$ each is a $(Q+1)\times(Q+1)$ matrix with the following elements:

$$U_{1qi}(K_T) = -\delta_{qi}\epsilon_q d\frac{\cot K_{x2q}s}{K_{x2q}} + \sum_{m=0}^{M}P_{im}P_{qm}\frac{\tan}{-\cot}\frac{K_{x1m}a_1}{\epsilon_m bK_{x1m}} \quad (22)$$

$$V_{1qi}(K_T) = \frac{\delta_{qi}\epsilon_q d}{K_{x2q}\sin K_{x2q}s} = -U_{2qi}(K_T) \quad (23)$$

$$V_{2qi}(K_T) = \delta_{qi}\epsilon_q d\frac{\cot K_{x2q}s}{K_{x2q}} - \sum_{l=0}^{L}P_{il}P_{ql}\frac{\cot K_{x3l}(a_1+s-a_2)}{\epsilon_l bK_{x3l}}. \quad (24)$$

The TE eigenvalues are therefore given by the roots of $\det[H]=0$ where $[H]$ is the following $2(Q+1)\times 2(Q+1)$ matrix:

$$[H(K_T)] = \left[\begin{array}{c|c} U_1 & V_1 \\ \hline U_2 & V_2 \end{array}\right]. \quad (25)$$

In the case of the TM modes one starts from the electric Hertzian vector and after the integral eigenvalue problem is formulated, the unknown aperture longitudinal electric fields are expanded as

$$E_{g_1}(y) = \sum_{i=1}^{I_1} C_i'\sin\frac{i\pi}{d}(y-a_3) \quad (26)$$

$$E_{g_2}(y) = \sum_{i=1}^{I_2} D_i'\sin\frac{i\pi}{d}(y-a_3). \quad (27)$$

The final matrix equations are similar to (20) and (21) and distinguishing the TM case by adding a prime, the matrix elements are given by

$$U'_{1qi}(K_T) = -\delta_{qi}\epsilon_q dK_{x2q}\cot K_{x2q}s - \sum_{m=1}^{M}P'_{im}P'_{qm}\frac{K_{x1m}}{\epsilon_m b}\frac{-\tan}{\cot}K_{x1m}a_1 \quad (28)$$

$$V'_{1qi}(K_T) = \delta_{qi}\epsilon_q d\frac{K_{x2q}}{\sin K_{x2q}s} = -U'_{2qi}(K_T) \quad (29)$$

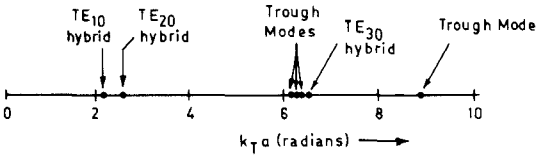

Fig. 2. The eigenvalue spectrum for a typical ridged waveguide with $b/a=0.5$, $c/a=0.5$, $d/b=0.125$, $s/a=0.125$, $h=h'$.

TABLE I
VARIATION OF DOMINANT TE EIGENVALUE WITH NUMBER OF GAP AND TROUGH FIELD TERMS (RIDGED WAVEGUIDE PARAMETERS: $b/a=0.5$; $c/a=0.5$; $d/b=0.5$; $s/a=0.125$;

Q	M	L	$K_T a$ (radians)
1	1	1	3.1868
1	5	5	2.9454
1	10	10	2.9361
1	20	20	2.9352
1	30	30	2.9349
5	5	5	2.9861
5	10	5	2.9703
5	10	10	2.9613
5	20	10	2.9596
5	20	20	2.9586
5	30	30	2.9579
10	10	10	2.9684
10	20	10	2.9661
10	20	20	2.9648
10	30	30	2.9618
15	15	15	2.9669
15	20	20	2.9657
15	30	30	2.9630

TABLE II
COMPUTED λ_c/a OF THE DOMINANT AND THE FIRST HIGHER ORDER TE MODES FOR $b/a=0.5$, $s/a=0.125$, AND $h=h'$ (JULL'S DATA FOR THE DOMINANT TE MODE ARE GIVEN IN PARENTHESES)

	c/a					
d/b	0.125	0.250	0.375	0.500	0.625	0.750
0.125	4.516 (4.47) 1.945	4.157 (4.12) 2.364	3.677 (3.72) 2.491	3.088 (3.20) 2.364	2.349 (2.40) 1.945	1.574 (1.58) 0.826
0.250	3.444 (3.481) 1.531	3.227 (3.283) 1.810	2.904 (3.001) 1.897	2.507 (2.629) 1.810	2.039 (2.076) 1.531	1.646 (1.649) 0.885
0.500	2.593 (2.620) 1.191	2.484 (2.5208) 1.342	2.316 (2.366) 1.391	2.117 (2.1649) 1.342	1.915 (1.910) 1.191	1.776 (1.7792) 0.942
0.750	2.195 (2.209) 1.043	2.145 (2.162) 1.105	2.076 (2.095) 1.128	2.002 (2.008) 1.105	1.935 (1.901) 1.043	1.891 (1.893) 0.971

and

$$V'_{2qi}(K_T)=\delta_{qi}\epsilon_q d K_{x2q}\cot K_{x2q}s - \sum_{l=1}^{L} P'_{il}P'_{ql}\frac{K_{x3l}}{\epsilon_l b}\cot K_{x3l}(a_1+s-a_2) \quad (30)$$

where

$$P'_{rs}=\int_{-a'_3}^{a_3}\sin\frac{r\pi}{d}(y-a_3)\sin\frac{s\pi}{b}(y-a_4)\,dy. \quad (31)$$

III. RESULTS OF NUMERICAL COMPUTATION

The characteristic equation $\det[H(k_T)]=0$ was solved iteratively to obtain the eigenvalue spectrum. The iteration scheme uses an incremental scanning initially to locate a change of sign, determines its nature and, if it is a zero, applies the standard secant method of iteration to determine the root. In Table I the convergence of the normalised eigenvalue $k_T a$ of the dominant TE mode with the number of gap and trough field terms—Q, M, L—is illustrated. The waveguide parameters are indicated in the table caption.

In Table II the normalised cutoff wavelengths λ_c/a of the dominant TE mode for various parameters, computed with $Q=M=L=10$, are given. Each value is followed by Jull's [4] theoretical data for extrapolated zero mesh limit in round brackets. The third entry in each square is λ_c/a of the next higher order TE mode which indicates the bandwidth characteristics for the particular ridge width chosen.

In Fig. 2 the first few TE eigenvalues of a ridged waveguide are indicated. It may be noted that the trough modes have not been assigned any modal designation. Unlike the case of a conventional ridged waveguide having one trough and one gap region, the trough mode designation in a waveguide with two double ridges does not follow a simple scheme, as in this case there are two different trough regions (I and III). A particular trough mode field pattern may consist of two different TE mode patterns in two trough regions leading to ambiguity in designation. For identifying the nature of field patterns without actually computing the field strength variations, the analysis was modified by introducing another symmetry plane along X-axis corresponding to symmetric ridges and the eigenvalues were scanned for different combination of X- and Y-symmetries. These, together with the approximate calculations based on the rectangular dimensions of the trough regions, give us an idea about the field patterns.

IV. CONCLUSIONS

The eigenvalue spectrum of rectangular waveguide with two symmetrically placed double ridges has been determined. The dominant mode results compare very well with Jull's [4] data obtained by finite difference technique. The bandwidth characteristics of the waveguide make it suitable for the varactor-tuned solid-state oscillators using waveguide resonators where full-height post mounting of devices leads to restricted tunability due to frequency

saturation. The evaluation of this waveguide for such applications would in turn require determination of the equivalent circuit of the ridge–gap mounting structure. That would be the topic of a future communication.

ACKNOWLEDGMENT

The authors are indebted to Prof. B. R. Nag for his helpful suggestions and critical appraisal of the manuscript. Thanks are also due to the Computer Centre, University of Calcutta, for providing the computing facilities.

REFERENCES

[1] S. B. Cohn, "Properties of Ridge Wave Guide," *Proc. IRE*, vol. 35, pp. 783–788, Aug. 1947.
[2] S. Hopfer, "The design of Ridged Waveguides," *IRE Trans. Microwave Theory Tech.*, vol. MTT-3, pp. 20–29, Oct. 1955.
[3] W. J. Getsinger, "Ridge Waveguide Field Description and Applications to Directional Couplers", *IRE Trans. Microwave Theory Tech.*, vol. MTT-10, pp. 41–50, Jan. 1962.
[4] E. V. Jull, W. J. Bleackley, and M. M. Steen, "The Design of Waveguides with Symmetrically Placed Double Ridges," *IEEE Trans. Microwave Theory Tech.*, vol. MTT-17, pp. 397–399, July 1969.
[5] S. Mizushina and T. Ohsuka, "The Ridged-Waveguide-Cavity Gunn Oscillator for Wide-Band Tuning," *IEEE Trans. Microwave Theory Tech.*, vol. MTT-24, pp. 257–259, May 1976.
[6] S. Mizushina, N. Kuwabara, and H. Kondoh, "Theoretical Analysis of a Ridged-Waveguide Mounting Structure," *IEEE Trans. Microwave Theory Tech.*, vol. MTT-25, pp. 1131–1134, Dec. 1977.
[7] J. P. Montgomery, "On the Complete Eigenvalue Solution of Ridged Waveguide," *IEEE Trans. Microwave Theory Tech.*, vol. MTT-19, pp. 547–555, June 1971.

Asymmetric Realizations for Dual-Mode Bandpass Filters

RICHARD J. CAMERON AND JOHN DAVID RHODES, SENIOR MEMBER, IEEE

Abstract—**Two analytic synthesis techniques are presented for even-degree asymmetric dual-mode in-line prototype networks up to degree 14. Commencing with the coupling matrix for the double cross-coupled array, rotational transformations are applied to transform the matrix into the form required for the dual-mode in-line asymmetric structure. "Asymmetric" here means that the coupling elements (irises, screws) are unequal in value about the physical center of the filter. The necessity for these asymmetric solutions arose when it was discovered that it was impossible to realize certain useful transmission characteristics with the symmetric in-line structure, on account of their transmission zero pattern in the complex-plane representation of the transfer function. Furthermore, because the full coupling matrix is used instead of the even-mode matrix as with the symmetric solution, the asymmetric in-line realization process may be applied to electrically asymmetric matrices, such as those for single-ended filters for multiplexer applications. To demonstrate the validity of the theory, a practical model of each type of realization has been constructed and measured.**

I. INTRODUCTION

THE PROBLEM of converting the mathematical describing polynomials of the characteristics of a low-pass prototype filter network into a symmetric in-line dual-mode structure was first addressed by Atia and Williams [1]. Firstly an even-mode coupling matrix was synthesized, and then by iteratively rotating this matrix certain prescribed couplings were annihilated. The resulting matrix, when unfolded into the full coupling matrix, contains only those couplings that could be realized by a symmetric in-line dual mode structure, while retaining the original 2-port electrical parameters. More recently, the procedure of annihilating the couplings by iteration and optimization has been replaced by analytic techniques for even filter orders 6–12 inclusive [2]. These analytic techniques use as their base, the folded coupling matrix for the generalized low-pass cross-coupled network, the synthesis of which is described in [3]. Using these new procedures, the full coupling matrices for symmetric in-line dual-mode filters are easily and quickly generated from the describing polynomials.

The symmetric realizations however have restrictions. Firstly, the methods cannot be used for electrically asymmetric characteristics, such as those for multiplexer applications. Secondly, there does not appear to be a solution for 14th order characteristics, which occasionally do have application. Thirdly, for lower degree cases, certain characteristics which have particular patterns of transmission zeros as represented in the Argand diagram are unrealizable with a symmetric structure. A complete set of realizability conditions is given in [2].

It was these reasons that prompted a study to be made into solutions other than with symmetric structures. In fact two general types of asymmetric solution were discovered. The first is a general asymmetric solution which

Manuscript received May 19, 1980; revised August 28, 1980.
R. J. Cameron is with the European Space Research and Technology Centre, 2200 AG, Noordwijk, The Netherlands.
J. D. Rhodes is with the Department of Electrical and Electronic Engineering, The University, Leeds LS2 OJT, England.

0018-9480/81/0100-0051$00.75 ©1981 IEEE